Preliminary Study for Localizing *c*, *d* and *e* Waves in Photoplethysmogram Signals

Mohamed Elgendi, *Senior Member*

***Abstract*—An efficient and robust method based on two moving-average filters followed by a dynamic event-duration threshold was developed to locate *c*, *d* and *e* waves in the acceleration photoplethysmogram (APG) signals. This investigation was the first of its kind to locate *c*, *d* and *e* waves in subjects measured at rest and after exercise. The method detects *c*, *d* and *e* in arrhythmia APG signals that suffer from: 1) non-stationary effects and 2) low signal-to-noise ratios. The performance of the proposed method was tested on 27 records collected in normal and heat-stressed conditions, resulting in a 99.95% sensitivity and 98.35% positive predictivity.**

I. Introduction

Atherosclerosis, the underlying cause of coronary heart disease, can occur even in children and adolescents [1, 2]. This has led to the belief that the primary prevention of atherosclerosis should commence in childhood. Monitoring arterial vascular walls and risk factors, such as hypertension, hypercholesterolemia and other blood biochemical profiles, might help identify individuals with an increased risk of developing atherosclerosis in adulthood.

PPG and APG will be used as acronyms for photoplethysmogram and its second derivative based on the recommendation in [3].

Several epidemiological studies have demonstrated that the information extracted from the APG waveform is closely associated with age and other risk factors for atherosclerotic vascular disease [4-6].

As shown in Figure 1, the waveform of the APG consists of four systolic waves (*a*, *b*, *c* and *d*) and one diastolic wave (*e*) [7]. The height of each wave was measured from the baseline. The values above the baseline were considered positive and those under it negative.

Although the clinical significance of APG measurement is thoroughly discussed, there is still a lack of studies focusing on the automatic localization of *c*, *d* and *e* waves in APG signals. Therefore, this investigation is the first of its kind. It is aimed to develop a rapid and robust algorithm to detect *c*, *d* and *e* waves in APG signals, especially in a heat-stressed context.

II. PPG Dataset

There are no standard PPG databases available to evaluate the developed algorithms. However, Charles Darwin University has a PPG dataset measured at rest and after exercise. The PPG data were collected as a minor part of a joint project between Charles Darwin University, the Defence Science and Technology Organisation (DSTO) and the Department of Defence. The background of the entire project can be found in [8].

The PPGs of 27 healthy male subjects with a mean ± SD age of 27 ± 6.9 were measured using a photoplethysmogram (Salus PPG), with the sensor located at the cuticle of the second digit of the left hand. The measurements were taken while the subject was at rest and after exercise on a chair. The PPG data were collected at a sampling rate of 200 Hz. The duration of each data segment was 20 seconds.

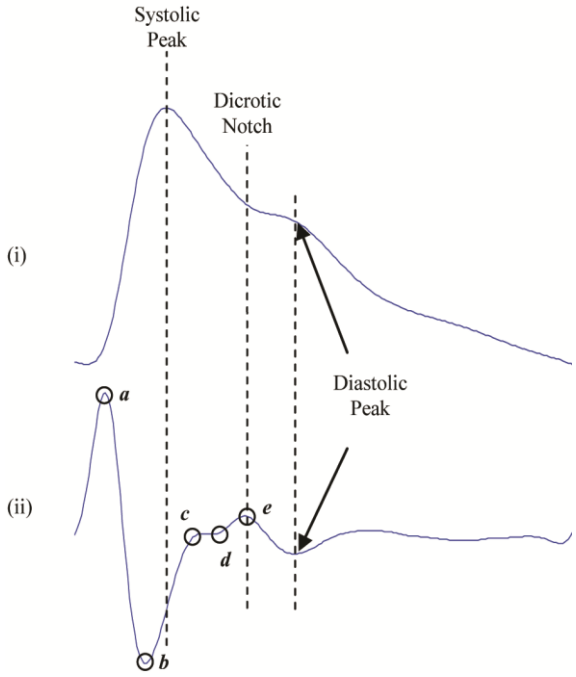

Figure 1. Signal Measurements [9] (i) fingertip photoplethysmogram; (ii) second derivative wave of photoplethysmogram

III. Methodology

The proposed *c, e* and *d* waves detection algorithm consists of three main stages: pre-processing (bandpass filtering, second derivative and squaring), feature extraction (generating potential blocks using two moving averages) and classification (thresholding).

Mohamed Elgendi is with the School of Computing Science, University of Alberta, Edmonton, Canada AB T6G 2E850, Email: moe.elgendi@gmail.com , Tel: +17808074141

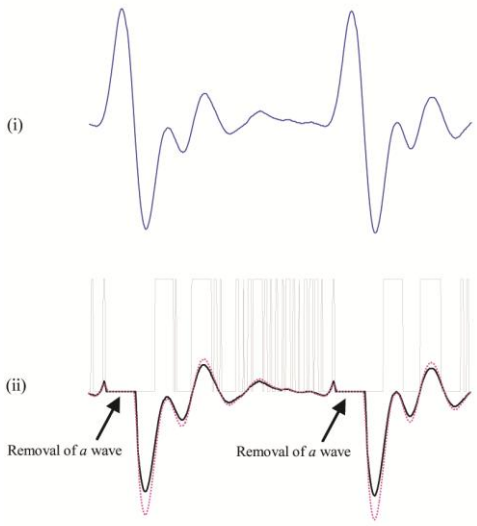

Figure 2. Demonstrating the effectiveness of using two moving averages to detect *c*, *d* and *e* waves (i) filtered APG signal with Butterworth bandpass filter; (ii) generating blocks of interest after using two moving averages; dotted line is the first moving average and the solid line is the second moving average

Bandpass filter

The quality of the PPG signal depends on the location and the properties of the subject's skin at measurement, including the individual skin structure, blood oxygen saturation, blood flow rate, skin temperatures and the measuring environment.

These factors generate several types of additive artifacts, which may be contained within the PPG signals. This may affect the extraction of features and, hence, the overall diagnosis, especially when the PPG signal and its derivatives will be assessed in an algorithmic fashion. The main challenges in processing the PPG signals are: power interference, motion artifact and low amplitude signals.

To design an efficient bandpass filter, two types of challenging noise must be addressed:

i) **High-frequency noise**: As discussed above, this noise could be created by the instrumentation amplifiers, the recording system pickup of ambient electromagnetic signals or other noises above 7 Hz. High-frequency noise is usually caused by interference from main power sources induced onto the recording leads of the PPG. This phenomenon introduces a sinusoidal component into the recording. In Australia, this component is at a frequency of 50 Hz.

ii) **Low-frequency noise**: As discussed, this noise is created by poor contact to the fingertip photo sensor. In addition, variations in temperature and bias in the instrumentation amplifiers can cause baseline drift. Regarding the PPG databases used in this work, the body movement was limited by short measurement time (20 s) and the fixed position of the arm during the PPG signal collection. The low-frequency noise can be removed using a high-pass filter. The low frequencies that cause baseline wandering exist up to 0.5 Hz.

The periodic interference is clearly displayed as a spike, not only at its fundamental frequency of 50 Hz, but also as spikes at 100 Hz and higher harmonics.

The main energy of *a* and *b* waves can be extracted using a bandpass filter, typically a bidirectional Butterworth implementation [10], as it offers good transition-band characteristics at low coefficient orders making it efficient to implement [10].

A second-order Butterworth filter with bandpass 1−7 Hz was implemented by cascading high- and low-pass filters to remove the baseline wander and high frequencies that did not contribute to the *a* and *b* waves. Since one complete heart cycle takes approximately 1 second, frequencies below 1 Hz were considered noise (baseline wander). The 7 Hz was chosen because most of the energy of the PPG signal is below 7 Hz.

Second derivative

To obtain the APG signals $Z[n]$, the second derivative was applied to the filtered PPG $S[n]$ to analyze the APG signals. It represented a non-causal filter with three-point center derivative, which created a delay of only two samples as follows:

$$S'[n] = \left.\frac{dS}{dt}\right|_{t=nT} = \frac{1}{2T}(S[n+1] - S[n-1])$$

$$Z[n] = \left.\frac{dS'}{dt}\right|_{t=nT} = \frac{1}{2T}(S'[n+1] - S'[n-1]) \quad ,$$

where T is the sampling interval and equals the reciprocal of the sampling frequency, and n is the number of data points.

b wave cancellation

At this stage, the *a* wave of the APG needed to be emphasized to distinguish it clearly for detection. This was done by setting the negative parts of the signal equal to zero.

a wave removal

To boost *c* and *d* waves to dominant features in the APG signal, the *a* wave was removed. This was done by setting the $Z[n]$ signal to zero for the duration of the *a* wave, producing signal $y[n]$. Figure 2 (ii) show the result of removing the *a* wave from the filtered signal of Figure 2 (i).

Generating blocks of interest

This metodology is based on Elgendi's methodlogy [11-14] for detecting *a* and *b* waves in APG signals using two moving averages. However, here the *c*, *d* and *e* waves will be detected instead of the *a* wave. Thus, the duration of the first moving average will be related to the minimum duration of the *c, d* and *e* waves, which is about 8 ms, while the duration of the second moving average will be related the average lenght of the *ced* segment, which is about 40 ms, as follows:

i) First moving average: The first moving average, shown as the dotted line in Figure 2 (ii), was used to detect the peaks of the *c* and *d* waves.

$$MA_{Peak}[n] = \frac{1}{W_1}(y[n-(W_1-1)/2] + ... + y[n] + ... + y[n+(W_1-1)/2])$$

where $W_1 = 8\,\text{ms} * SF$, which is the average duration for *c*, *d* and *e* waves, rounded to the nearest odd integer.

ii) Second moving average: This was used as a threshold for the first moving average, and is shown as a solid line in Figure 2 (ii) as follows:

$$MA_{CED\ Segment}[n] = \frac{1}{W_2}(y[n-(W_2-1)/2] + ... + y[n] + ... + y[n+(W_2-1)/2])$$

where $W_2 = 40\,\text{ms} * SF$, which is the average duration for the *ced* segment, rounded to the nearest odd integer.

Blocks of interest are generated when the amplitude of the first moving-average filter (MA_{Peak}) was greater than the amplitude of the second moving-average filter, then ($MA_{CEDsegment}$).

Thresholding

Blocks with a smaller width than the average window size of the *c*, *d* or *e* peak (W_1) were considered noisy blocks and rejected. The expected size for the *c*, *d* or *e* peak is based on observational statistics for healthy adults, which varies from 6 ms to 10 ms based on

$$peak\_Blocksize = (a_i a_{i+1}/SF) * W_1,$$

where $a_i a_{i+1}$ is the *aa* interval that contains the blocks of interest and *SF* is the sampling frequency.

To determine whether the detected blocks contain *c*, *d* or *e* waves, the number of blocks in each consecutive *aa* interval was first counted. A threshold was then applied based on the distance of the maximum point within a block to the *a* peak to distinguish *c* waves from *e* waves and noise.

There were two possibilities for the number of detected blocks:

1. More than one block: The distance of the maximum point within a block to the nearest *a* peak will be used as a measure for selecting the blocks that contain potential *c*, *e* or *d* waves. This consists of two steps:
   i. *Detect potential c and e waves*. A block would be considered to contain a *c* wave if the distance of the maximum point of the block to the nearest *a* peak was within a certain range. The maximum absolute value within the first accepted block at the right-hand side of the *b* wave was considered the *c* peak. The maximum absolute value of the second accepted block after the *c* peak was considered the *e* peak. Usually, the *c*, *e* and *d* waves did exist in APG signals measured at rest as shown in Figure 3 (i).
   ii. *Detect d waves*. The minimum value that lies between the *c* peak and the *e* peak was considered the *d* peak, as shown in Figure 3 (i).
2. One block: The *c* and *e* waves were most likely merged within one block, which was marked with a ⊕ symbol, as shown in Figure 3 (ii). The *c*, *e* and *d* waves were usually merged in APG signals measured after exercise.

The detected waves were compared to the annotated waves file to determine whether the *c*, *d* and *e* waves were detected correctly.

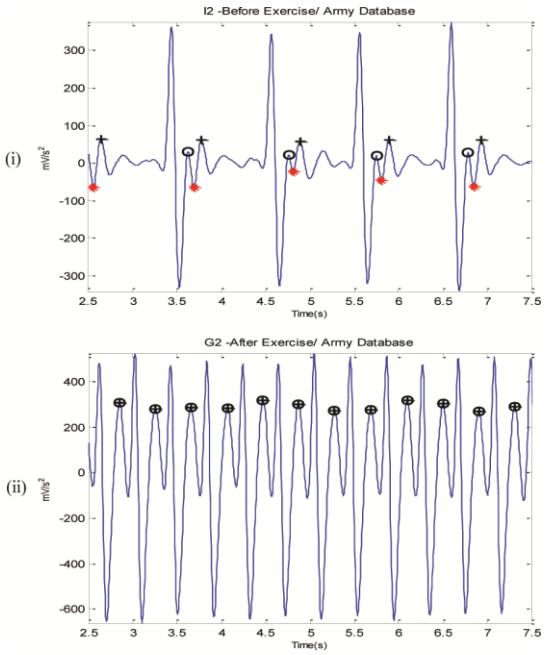

Figure 3. Detected *c*, *d* and *e* waves in APG signals (i) at rest and (ii) after exercise; 'O' represents the *c* wave; '*' represents the *d* wave; '+' represents the *e* wave; I2 and G2 refer to the subject ID.

IV. Discussion

As mentioned, the main objective behind testing the algorithm against the APG measured after exercise was to test the robustness of the algorithm against non-stationary effects, low signal-to-noise-ratio (SNR) and a high heart rate. All of the reasons for detection failure are described below.

1) Stationarity. The APG signals for subjects I2 (before exercise) and G2 (after exercise) were stationary. The proposed algorithm detected the *c, d* and *e* waves correctly in stationary APG signals as shown in Figure 3(i) and Figure 3(ii). However, the *c, d* and *e* waves are merged in Figure 3 (ii) because of the high heart rate of the subject.

2) Low amplitude. The APG signals of subjects O2 (before exercise) and B2 (after exercise) had low amplitude. The proposed algorithm handled low APG waves amplitude.

3) Non-stationarity. The proposed algorithm detected the *c, d* and *e* waves correctly in non-stationary APG signals.

4) Regular heart rhythm. The proposed algorithm detected the *c, d* and *e* waves correctly in APG signals with regular heart rhythms, as shown in Figures 3(i) and 3(ii).

5) High-frequency noise. The proposed algorithm was very robust at detecting noise for subjects Q1 (before exercise) and A1 (after exercise).

Although the duration of the *c, d* and *e* waves changed dramatically after exercise, the proposed algorithm succeeded in detecting the *c, d* and *e* waves efficiently as shown in Tables 1 and 2.

TABLE I
PERFORMANCE OF THE *C*, *D* AND *E* WAVES DETECTION ALGORITHMS ON APG SIGNALS MEASURED AT REST

	At Rest (Before Exercise)					
	No of beats	**TP**	**FP**	**FN**	**Se (%)**	**+P (%)**
c wave detection	584	577	7	0	100.0	98.97
d wave detection		571	13	0	100.0	97.81
e wave detection		582	2	0	100.0	99.68

TABLE II
PERFORMANCE OF THE *C*, *D* AND *E* WAVES DETECTION ALGORITHMS ON APG SIGNALS MEASURED AFTER EXERCISE

	After Exercise					
	No of beats	**TP**	**FP**	**FN**	**Se (%)**	**+P (%)**
c wave detection	885	848	36	0	100.0	95.98
d wave detection		875	10	0	100.0	98.66
e wave detection		874	10	3	99.70	99.01

Few false negatives occurred in subjects N3 and B2 measured after exercise; this is because the *e* wave was not salient enough to be detected. Due to high noise in the APG signals, a number of false positives occurred. However, the number of false positives in the detection of the *c* waves was the highest because of its morphology and small duration.

As mentioned, the main objective behind testing the algorithm against the APG measured after exercise was to test the robustness of the algorithm against non-stationary effects, low SNR and high heart rate. All of the reasons for detection failure are described below.

V. CONCLUSION

Most research relating to the APG was done in Japan. In addition to cardiovascular risk factors, the APG has been described as a potential diagnostic tool for a wide variety of other problems and disorders, such as sensations of coldness, stress experienced by surgeons, exposure to pneumonia, intracerebral hemorrhage and acute poisoning.

Currently a full understanding of the diagnostic value of the different features of the PPG signal is still lacking and more research is needed. Moreover, there has been very little research done on the detection algorithm of *c*, *d* and *e* waves in APG signals.

However, a promising algorithm was proposed to detect *c*, *d* and *e* waves simulternously and robustly against high-frequency noise, low amplitude, non-stationary effects and irregular heartbeats in APG signals measured before and after exercise. This numerically-efficient algorithm was evaluated using 27 records, containing 1,469 heartbeats, and resulting in 99.95% sensitivity and 98.35% positive predictivity.

ACKNOWLEDGMENTS

Mohamed Elgendi would like to gratefully acknowledge the Australian government and Charles Darwin University, whose generous scholarships facilitated this research. He would also like to thank Prof. Friso De Boer for his valuable comments.

REFERENCES

[1] P. G. Kimm SY, Stylianou MP, Waclawiw MA, Lichtenstein C "National trends in the management of cardiovascular disease risk factors in children: second NHLBI survey of primary care physicians," *Pediatrics,* p. 102:E50, 1998.

[2] M. G. Strong JP, McMahan CA, Tracy RE, Newman WP, Herderick EE, Cornhill JF . "Prevalence and extent of atherosclerosis in adolescents and young adults. Implications for prevention from the pathobiological determinants of atherosclerosis in young study," *JAMA* pp. 281:727-737, 1999.

[3] M. Elgendi, "Standard Terminologies for Photoplethysmogram Signals," *Current Cardiology Reviews,* vol. 8, pp. 215-219, 2012.

[4] W. K. Takada H, Harrel JS, Iwata H "Acceleration plethysmography to evaluate aging effect in cardiovascular system. Using new criteria of four wave patterns. ," *Medical Progress through Technology,* pp. 21:205-210, 1996.

[5] H. H. Imanaga I, Koyanagi S, Tanaka K " Correlation between wave components of the second derivative of plethysmogram and arterial distensibility.," *Jpn Heart J* pp. 39:775-784, 1998.

[6] T. N. Takazawa K, Fujita M, Matsuoka O, Saiki T, Aikawa M, Tamura S, Ibukiyama C, "Assessment of vascular agents and vascular aging by the second derivative of photoplethysmogram waveform," *Hypertension,* pp. 32:365-370, 1998.

[7] F. M. Takazawa K, Kiyoshi Y, Sakai T, Kobayashi T, Maeda K, Yamashita Y, Hase M, Ibukiyama C, "Clinical usefulness of the second derivative of a plethysmogram (acceralation plethysmogram)," *Cardiology,* pp. 23:207-217, 1993.

[8] A. Matsuyama, "ECG and APG Signal Analysis during Exercise in a Hot Environment," PhD, School of Engineering and Information Technology, Charles Darwin University, Darwin, Australia, 2009.

[9] M. Elgendi, "On the Analysis of Fingertip Photoplethysmogram Signals," *Current Cardiology Reviews,* vol. 8, pp. 14-25, 2012.

[10] A. Oppenheim and R. Shafer, *Discrete-time Signal Processing*. NJ: Prentice Hall, 1989.

[11] M. Elgendi*, et al.*, "Measurement of a-a Intervals at Rest in the Second Derivative Plethysmogram," presented at the IEEE Conference in Bioelectronics and Bioinformatics, RMIT University, Melbourne, 2009.

[12] M. Elgendi*, et al.*, "Heart Rate Variability Measurement Using the Second Derivative Photoplethysmogram," presented at the The 3rd International Conference on Bio-inspired Systems and Signal Processing (BIOSIGNALS2010), Spain, 2010.

[13] M. Elgendi*, et al.*, "Heart Rate Variability and Acceleration Plethysmogram measured at rest," in *Biomedical Engineering Systems and Technologies*, A. Fred*, et al.*, Eds., ed: Springer, 2011, pp. 266-277.

[14] M. Elgendi*, et al.*, "Applying the APG to measure Heart Rate Variability," in *The 2nd International Conference on Computer and Automation Engineering*, Singapore, 2010, pp. 100-104.